Apparent-Mass Coefficients for Isosceles Triangles and Cross Sections Formed by Two Circles

Ming-Ke Huang* and Chuen-Yen Chow†
University of Colorado, Boulder, Colorado

In applying inviscid slender-body theory to the calculation of aerodynamic forces on two special types of fuselage, conformal mapping techniques are used to find the exact expressions for the apparent-mass coefficients of their cross sections. The fuselage cross sections considered here either are formed by two circular arcs or have the shape of isosceles triangles. The exact solutions are used to check the applicability of approximating methods using area-equivalence, width-equivalence, and height-equivalence rules. It is found that the area-equivalence rule can hardly be used to estimate the normal forces on all of the cross sections considered in this paper.

Introduction

ACCORDING to the inviscid slender-body theory, the lift and sideforce acting on a body can be computed if the apparent-mass coefficients for sections along that body are known. Those coefficients for a large variety of body shapes that are useful in airplane and missile designs have been tabulated in Table 10.3 of Ref. 1 and in Table 1 of Ref. 2. Concerning especially wing-fuselage combinations, authors of Refs. 3-7 have obtained the coefficients for a number of cross-sectional shapes in that category. It is shown in the present work that additional analytic expressions for apparent-mass coefficients can be derived for two types of fuselage without a wing, whose cross sections either are formed by two circular arcs or have the shape of isosceles triangles.

Computation of the sectional properties of a body of arbitrary configuration is usually tedious. Approximating methods are sometimes used in the early stage of aircraft design to estimate the aerodynamic forces acting on various components of an aircraft.

One method based on the area-equivalence (A-E) rule is to approximate the actual slender body by an equivalent body of revolution having the same area distribution[8]; aerodynamic forces on the approximated body of circular cross sections can be calculated using well-known formulas.[9] On the other hand, if the body is approximated by a body of revolution having the same width in lift computations, the approximation is called the width-equivalence (W-E) rule. It is called the height-equivalence (H-E) rule in sideforce computations when the approximated circular cylinder has the same height distribution as the original.

It is known that the W-E and H-E rules correctly determine the apparent-mass coefficients for calculating the lift and sideforce on a body having either elliptical or flat-plate cross sections.[1] When these and the A-E rule are applied on bodies of other cross-sectional shapes, errors are expected in the results. Since exact expressions for apparent-mass coefficients are obtained in this paper for some special cross sections, applicability of the aforementioned approximating methods is tested on those configurations.

Apparent-Mass Coefficients in Slender-Body Theory

The method using apparent masses to compute aerodynamic forces and moments on a slender body was suggested by Jones,[10] generalized by Bryson,[11] and later summarized by Nielsen.[1] The procedure for computation is outlined here for a simplified case of a slender body moving steadily without angular motions through an incompressible fluid, as sketched in Fig. 1. The body is performing a translational motion with a constant speed U along the horizontal x axis. If the body axis makes a small angle of attack α with the flight direction on the x-z plane to a cross section on the body, the surrounding fluid is moving at a relative speed $v_2 (\cong U\alpha)$ in the positive z direction. Similarly, if the body axis makes a sideslip angle β (not shown in the figure) with U on the x-y plane, a relative side motion $v_1 (\cong U\beta)$ is induced in the y direction. For small angles, the area of a cross section on the y-z plane can be approximated by that perpendicular to the body axis at the same axial position.

Let the kinetic energy of the fluid per unit length in the x direction be expressed as

$$T = \tfrac{1}{2} m_{11} v_1^2 + m_{12} v_1 v_2 + \tfrac{1}{2} m_{22} v_2^2 \tag{1}$$

where m_{ij} are called the apparent-mass coefficients, having the property that $m_{12} = m_{21}$. Aerodynamic forces appear on a fuselage of varying sectional properties. The lift and sideforce per unit axial length of the body are related to the apparent-mass coefficients through the following formulas:

$$Z = U^2 \alpha \frac{\mathrm{d}}{\mathrm{d}x} (m_{21} + m_{22}) \tag{2}$$

$$Y = U^2 \beta \frac{\mathrm{d}}{\mathrm{d}x} (m_{11} + m_{12}) \tag{3}$$

Let $\zeta = y + iz$ be a complex variable, $W_1(\zeta)$ be the complex potential of the flow caused by a uniform stream of unit speed moving toward the section along the positive y axis, and $W_2(\zeta)$ be the complex potential of a similar flow moving along the positive z axis. After the complex potentials become known, the apparent-mass coefficients can be computed as follows:

$$m_{11} + i m_{12} = i\rho \oint_c W_1 \mathrm{d}\zeta - \rho S \tag{4}$$

$$m_{21} + i m_{22} = i\rho \oint_c W_2 \mathrm{d}\zeta - i\rho S \tag{5}$$

in which ρ is the fluid density, S is the cross-sectional area of the body in the cross-flow plane, and the path of integration c is along the periphery of the body cross section following a counterclockwise direction in the y-z plane.

Received Sept. 3, 1982; revision received Nov. 26, 1982.

*Visiting Associate Professor, Dept. of Aerospace Engineering Sciences; presently Associate Professor, Dept. of Aerodynamics, Nanjing Aeronautical Institute, Nanjing, China.

†Professor, Dept. of Aerospace Engineering Sciences. Associate Fellow AIAA.

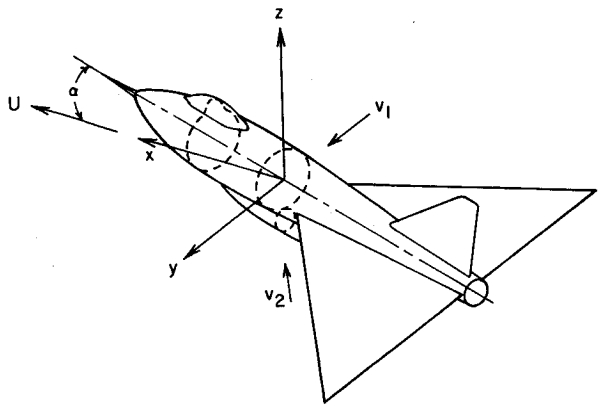

Fig. 1 Coordinate system for apparent-mass analysis.

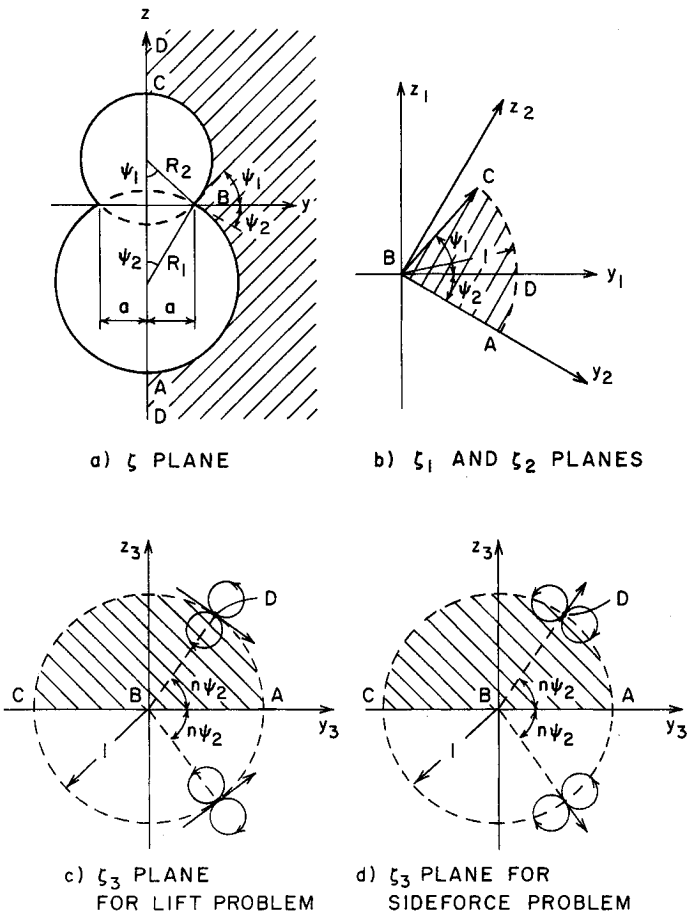

Fig. 2 Successive conformal mappings for sections formed by two circles.

For bodies whose cross sections are symmetric about the z axis, such as those dealt with in this paper, $m_{12}=m_{21}=0$ and the preceding formulas can be simplified accordingly.

Lift on Cross Sections Formed by Two Circles

We consider first a family of cross sections that are formed by two circles. The general configuration shown in Fig. 2a consists of two intersecting circles that are centered on the z axis and have radii R_1 and R_2, respectively. The tangents to the local circular arcs at the intersection B make angles ψ_1 and ψ_2, respectively, with the y axis. Various cross sections can be generated by adjusting the relative position and radii of these two circles, as will be seen later. In the lift problem the fluid motion far away from the body is along the z axis.

The complex potential W_2 in Eq. (5) for the lift problem can usually be written out if the body cross section can be mapped into a simple geometry through successive transformations. For the present case the fractional linear transformation

$$\zeta_1=(\zeta-a)/(\zeta+a) \tag{6}$$

is used as the first step. It maps the point B at $\zeta=a$ into the origin and the right half of the flowfield in the ζ plane into the interior of the fan-shaped region in the ζ_1 plane, as shown in Fig. 2b. This region is rotated through a counterclockwise angle ψ_2 in the ζ_2 plane, and is then mapped into a semicircle of unit radius shown in Fig. 2c, by the use of successive transformations

$$\zeta_2=\zeta_1 e^{i\psi_2} \tag{7}$$

$$\zeta_3=\zeta_2^n \tag{8}$$

where

$$n=\pi/(\psi_1+\psi_2) \tag{9}$$

The point D that represents infinity in the ζ plane is now mapped into a point at $\zeta_3=\exp(in\psi_2)$ on the periphery of the semicircle of unit radius in the ζ_3 plane.

The complex potential in the ζ_3 plane must satisfy the requirements that the resultant flow be tangent to both the straight line ABC (the body surface) and the arc CDA (part of the z axis outside the body in the physical plane); and that after being transformed back into the ζ plane, its far field represents a uniform stream of unit speed in the positive z direction. A potential flow that fulfills both tangential conditions can be constructed by adding a doublet of strength κ at D, with the doublet axis tangent to the local circular arc, and its mirror image with the y_3 axis as the mirror. Thus containing an undetermined strength κ, the complex potential of this flow is

$$W_2=W_{2A}+W_{2B}$$

$$=-\frac{\kappa\exp[-i(\pi/2-n\psi_2)]}{\zeta_3-\exp(in\psi_2)}-\frac{\kappa\exp[i(\pi/2-n\psi_2)]}{\zeta_3-\exp(-in\psi_2)} \tag{10}$$

We now show that when transformed into the ζ plane, this function describes a uniform flow at infinity. The right-hand side of Eq. (6) is first expanded in a series of negative powers of ζ, which is then substituted into Eqs. (7) and (8) to obtain a similar series expansion for ζ_3. By the use of the latter, the complex potential for the doublet at D, expressed by the first term on the right side of Eq. (10), becomes

$$W_{2A}=-\frac{i\kappa}{2an}\left(\zeta+an+\frac{(n^2-1)a^2}{3\zeta}+\ldots\right) \tag{11}$$

in which the first term represents a uniform flow parallel to the z axis, the second term is a constant that does not affect the magnitude of the velocity, and all terms thereafter are damped out at infinity. A similar expansion of the second term on the right side of Eq. (10), representing the complex potential for the image doublet, yields a series

$$W_{2B}=\frac{i\kappa\exp[i(\pi/2-n\psi_2)]}{2\sin(n\psi_2)}+\frac{i\kappa an}{2\sin^2(n\psi_2)}\frac{1}{\zeta}+\ldots \tag{12}$$

which has no influence at infinity. Thus, by requiring that the uniform stream in the physical plane be of unit speed, the doublet strength is found to be

$$\kappa=2an \tag{13}$$

The integral in Eq. (5) is evaluated by using the residue theorem after substitution of Eqs. (11) and (12) into the integrand. The result shows that the right-hand side of Eq. (5) is purely imaginary so that $m_{21}=0$. Dividing the imaginary part by $\rho\pi R_1^2$, we obtain a generalized expression for the non-vanishing apparent-mass coefficient in dimensionless form:

$$\frac{m_{22}}{\rho\pi R_1^2}=2\left(\frac{a}{R_1}\right)^2\left[\frac{1-n^2}{3}+\left(\frac{n}{\sin n\psi_2}\right)^2\right]-\frac{S}{\pi R_1^2} \tag{14}$$

For a circle of area S, the apparent-mass coefficient is ρS according to Table 10.3 of Ref. 1. Thus the A-E rule has the form

$$(m_{22}/\rho\pi R_1^2)_{AE}=S/\pi R_1^2 \tag{15}$$

For a circle whose diameter is equal to the maximum width R_1 of the original body cross section, the apparent-mass coefficient is $\rho\pi R_1^2$ so that the W-E rule becomes

$$(m_{22}/\rho\pi R_1^2)_{WE}=1 \tag{16}$$

Four different cross sections are generated by varying the geometric parameters of the two circles described in Fig. 2a.

A. Two Circles of Equal Radii

In this case $R_1=R_2=R$, $\psi_1=\psi_2=\psi$, and $n\psi_2=\pi/2$. The cross-sectional configuration is determined by the radius R and the distance $2h$ between the centers of these two circles. Having these two parameters specified, we can compute all other variables:

$$\psi=\cos^{-1}\frac{h}{R},\quad n=\frac{\pi}{2\psi},\quad \frac{S}{\pi R^2}=2-\frac{2}{\pi}\left[\psi-\frac{h}{R}\sqrt{1-\left(\frac{h}{R}\right)^2}\right] \tag{17}$$

Equation (14) is then reduced to

$$\frac{m_{22}}{\rho\pi R^2}=\frac{2}{3}(2n^2+1)\left[1-\left(\frac{h}{R}\right)^2\right]-\frac{S}{\pi R^2} \tag{18}$$

and is plotted in Fig. 3. The A-E rule, Eq. (15), together with the W-E rule, Eq. (16), are also plotted in the same figure.

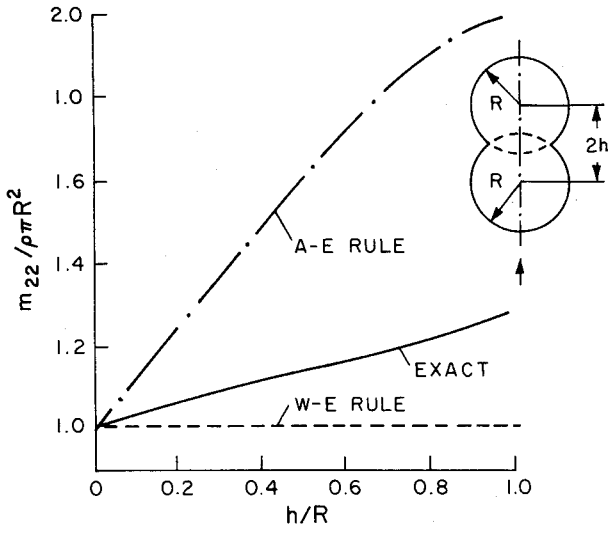

Fig. 3 Apparent-mass coefficient for sections formed by two circles of equal radii in lift problem.

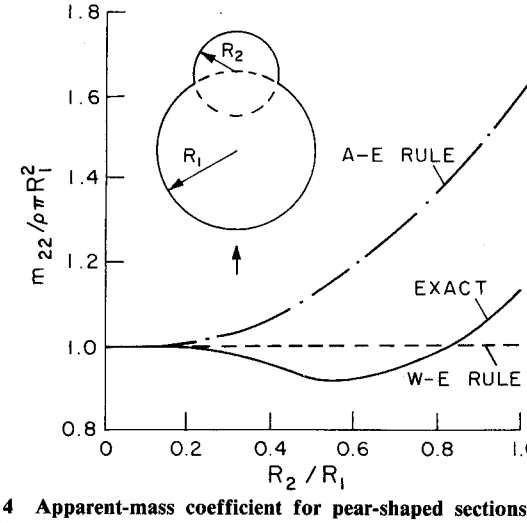

Fig. 4 Apparent-mass coefficient for pear-shaped sections in lift problem.

B. Center of One Circle on the Circumference of the Other Circle

The pear-shaped section so constructed, as shown in Fig. 4, may be used to approximate the portion of the fuselage containing the cockpit as sketched in Fig. 1. In this case,

$$\frac{S}{\pi R_1^2}=1+\left(\frac{R_2}{R_1}\right)^2-\frac{1}{\pi}\left[\left(\frac{R_2}{R_1}\right)^2\psi_1+\psi_2\right]+\frac{a}{\pi R_1}\left(\frac{R_2}{R_1}\cos\psi_1+\cos\psi_2\right) \tag{19}$$

The computational procedure is as follows. For given values of R_1 and a, we first calculate ψ_2, ψ_1, and R_2 using geometric relations

$$\sin\psi_2=\frac{a}{R_1}\qquad \cot\psi_1=\frac{R_1}{a}-\cot\psi_2\qquad R_2=\frac{a}{\sin\psi_1} \tag{20}$$

and then obtain the value of n using Eq. (9). Curves based on Eqs. (14-16) are plotted in Fig. 4.

C. Two Tangent Circles

This arrangement approximately describes the body-store or body-engine configuration of an airplane (Fig. 1). It is a special case obtained by letting $a\to 0$ in Fig. 2a. Referring to that figure, we have $a=R_1\psi_2=R_2\psi_1$ as $a\to 0$. It can readily be shown from Eq. (9) and from the geometry that

$$na=\frac{\pi R_1R_2}{R_1+R_2}\qquad n\psi_2=\frac{\pi R_2}{R_1+R_2}\qquad \frac{S}{\pi R_1^2}=1+\left(\frac{R_2}{R_1}\right)^2 \tag{21}$$

Use of these relations in Eq. (14) yields

$$\frac{m_{22}}{\rho\pi R_1^2}=2\left(\frac{\pi R_2/R_1}{1+R_2/R_1}\right)^2\left[\frac{2}{3}+\cot^2\left(\frac{\pi}{1+R_2/R_1}\right)\right]-\left[1+\left(\frac{R_2}{R_1}\right)^2\right] \tag{22}$$

Resultant curves for this case are plotted in Fig. 5.

D. A Partial Circle with a Flat Top

If we let $\psi_1=\pi$, the upper circle in Fig. 2a is flattened to become a line segment on the y axis. Thus, letting $R_1=R$ and $\psi_2=\psi$, we have

$$\psi=\cos^{-1}\frac{h}{R},\quad n=\frac{\pi}{\pi+\psi},\quad \frac{S}{\pi R^2}=1-\frac{1}{\pi}\left[\psi-\frac{h}{R}\sqrt{1-\left(\frac{h}{R}\right)^2}\right] \tag{23}$$

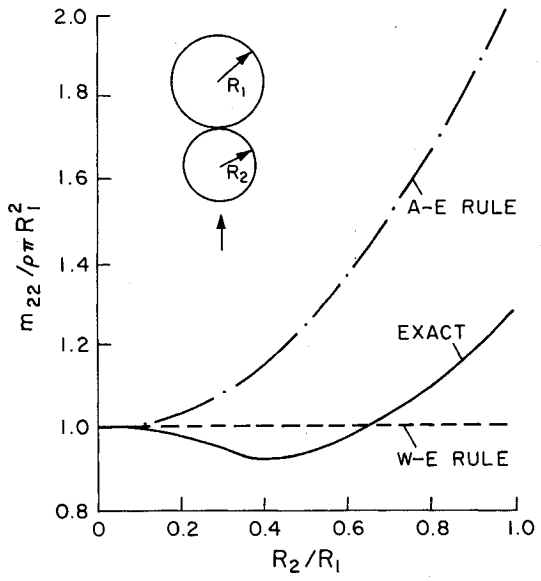

Fig. 5 Apparent-mass coefficient for body-store sections in lift problem.

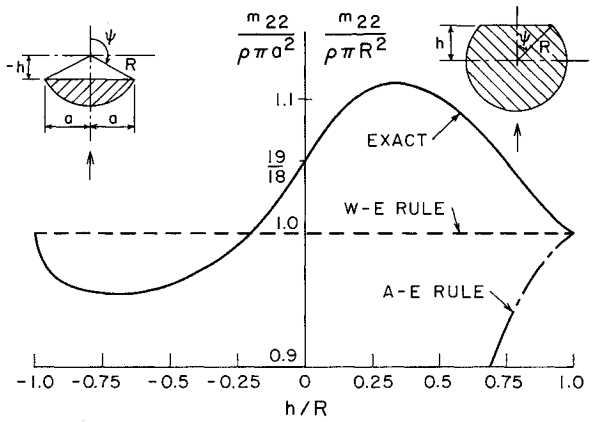

Fig. 6 Apparent-mass coefficient for flat-topped partial circular sections in lift problem.

in which h is the height of the flat top above the center of the circle of radius R, as sketched on the right side of Fig. 6.

For positive values of h, Eq. (14) becomes

$$\frac{m_{22}}{\rho\pi R^2} = 2\sin^2\psi\left[\frac{1-n^2}{3} + \left(\frac{n}{\sin n\psi}\right)^2\right] - \frac{S}{\pi R^2} \tag{24}$$

which is plotted on the right half of that figure. However, for negative values of h the cross section has the form as sketched on the left side of Fig. 6, for which a ($=R\sin\psi$) instead of R is the proper reference width. The variation of $m_{22}/\rho\pi a^2$ with negative h/R is plotted on the left half of Fig. 6. The dimensionless apparent-mass coefficient according to the W-E rule has a constant value of unity for all values of h/R. On the other hand, the A-E rule gives a curve so steep that only a small part of it appears in the figure.

Sideforce on Cross Sections Formed by Two Circles

We now compute the apparent-mass coefficients for the four body sections just considered when the flow faraway is in the y direction. Those coefficients, to be determined by the complex potential W_1 through Eq. (4), are needed in Eq. (3) for sideforce computations.

The conformal mapping procedures for the present problem are the same as those described in Fig. 2. However, the boundary conditions are somewhat different from those in the lift problem. In the physical ζ plane the flow must be tangent to the body surface ABC, but be normal to the parts of the z axis that are outside the body. After being mapped into the ζ_3 plane, these conditions become that the flow be tangent to the straight line ABC and be normal to the semicircular arc CDA. Both requirements are satisfied if a doublet of strength κ, whose axis is in the radial direction, is placed at point D and its image is placed at the corresponding position below the mirror ABC, as shown in Fig. 2d. The resultant flow is automatically normal to the unit circle since that circle is an equipotential line shared by both doublets. The complex potential in the ζ_3 plane is the sum of the complex potentials of these two doublets:

$$W_1 = W_{1A} + W_{1B} = \frac{\kappa\exp(in\psi_2)}{\zeta_3 - \exp(in\psi_2)} + \frac{\kappa\exp(-in\psi_2)}{\zeta_3 - \exp(-in\psi_2)} \tag{25}$$

Expressing the contributing complex potentials in powers of ζ similar to the form of expressions (11) and (12), we can show that at a faraway distance the doublet at D transforms into a horizontal flow in the physical plane, whose speed becomes unity if the doublet strength is still determined by Eq. (13), and the effect of the image doublet diminishes with increasing distance as $1/\zeta$. After evaluation of the integral on its right-hand side, Eq. (4) shows that $m_{12}=0$ and, closely resembling Eq. (14) in appearance, the real part is

$$\frac{m_{11}}{\rho\pi R_1^2} = 2\left(\frac{a}{R_1}\right)^2\left[\frac{n^2-1}{3} + \left(\frac{n}{\sin n\psi_2}\right)^2\right] - \frac{S}{\pi R_1^2} \tag{26}$$

The A-E rule is the same as that described by Eq. (15) for the lift problem,

$$(m_{11}/\rho\pi R_1^2)_{AE} = S/\pi R_1^2 \tag{27}$$

but the H-E rule is different and has the form

$$(m_{11}/\rho\pi R_1^2)_{HE} = (H/R_1)^2 \tag{28}$$

where H represents the height of the cross section measured in the z direction.

These general formulations are applied again to the four cross sections considered previously in the lift problem. Various forms of Eq. (26) are, for the case of two circles of equal radii,

$$\frac{m_{11}}{\rho\pi R_1^2} = \frac{2}{3}(4n^2-1)\left[1-\left(\frac{h}{R}\right)^2\right] - \frac{S}{\pi R^2} \tag{29}$$

for the case of two tangent circles,

$$\frac{m_{11}}{\rho\pi R_1^2} = 2\left(\frac{\pi R_2/R_1}{1+R_2/R_1}\right)^2\left[\frac{4}{3} + \cot^2\left(\frac{\pi}{1+R_2/R_1}\right)\right] - \left[1+\left(\frac{R_2}{R_1}\right)^2\right] \tag{30}$$

and, for the case of a partial circle with a flat top,

$$\frac{m_{11}}{\rho\pi R^2} = 2\sin^2\psi\left[\frac{n^2-1}{3} + \left(\frac{n}{\sin n\psi}\right)^2\right] - \frac{S}{\pi R^2} \tag{31}$$

Expressions for the cross-sectional area of these configurations have already been shown in the preceding section.

Results for the cross-flow problem are plotted in Figs. 7-10 in comparison with those obtained using A-E and H-E rules.

Lift and Sideforce on Isosceles Triangular Cross Sections

An isosceles triangle of half vertex angle θ and of base length $2a$ is shown in the ζ ($=r+is$) plane of Fig. 11a. The

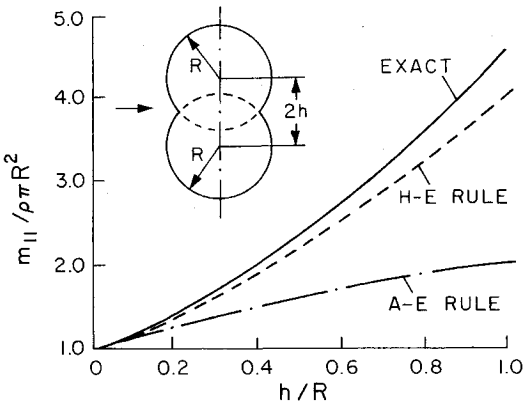

Fig. 7 Apparent-mass coefficient for sections formed by two circles of equal radii in sideforce problem.

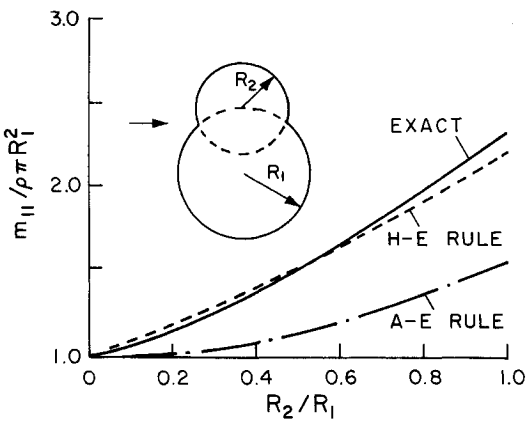

Fig. 8 Apparent-mass coefficient for pear-shaped sections in sideforce problem.

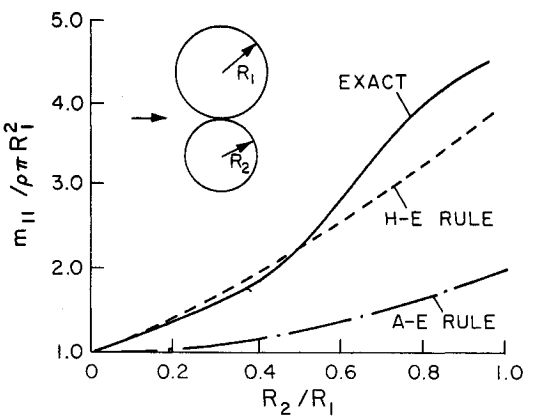

Fig. 9 Apparent-mass coefficient for body-store sections in sideforce problem.

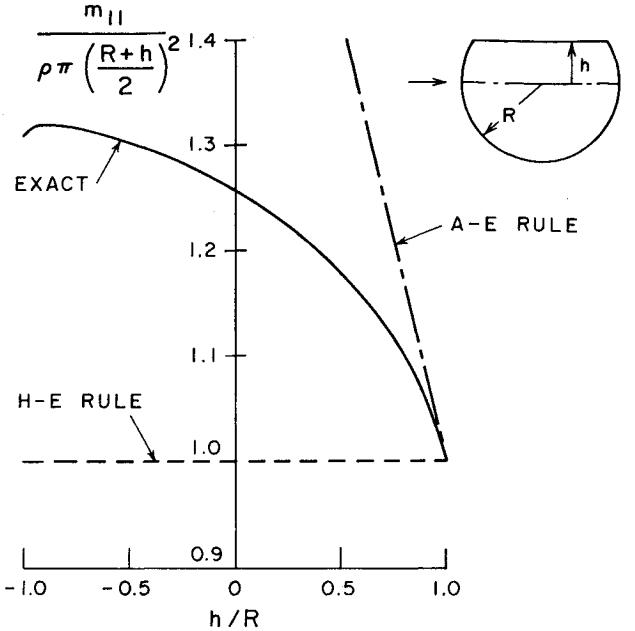

Fig. 10 Apparent-mass coefficient for flat-topped partial circular sections in sideforce problem.

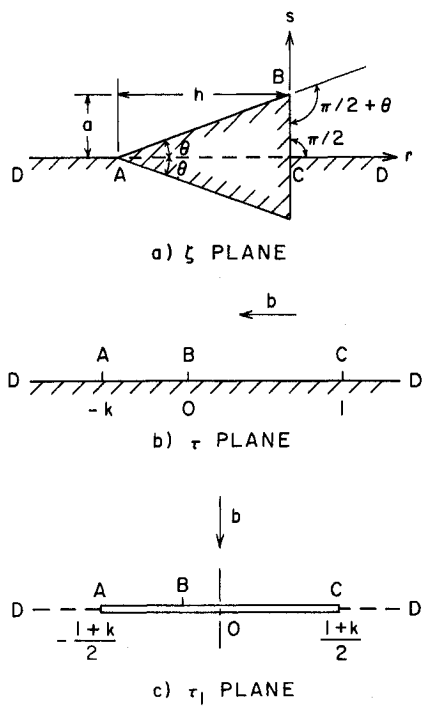

Fig. 11 Successive conformal mappings for isosceles triangular sections.

triangle has been rotated 90 deg from its orientation in the physical y-z plane to facilitate conformal mapping procedures. Because of symmetry, only the upper half of the flowfield needs to be considered.

In the lift problem the line DCBAD is a streamline. It is mapped into the real axis of the τ plane, shown in Fig. 11b, by the Schwarz-Christoffel transformation

$$\zeta = b\int_0^{\tau} (\tau+k)^{-\theta/\pi}\tau^{1/2+\theta/\pi}(\tau-1)^{-1/2}\,d\tau + ia \tag{32}$$

in which b and k are constants to be determined. The derivative of this information can be expanded in negative powers of τ:

$$\frac{d\zeta}{d\tau} = b\left\{1+\left(\frac{1}{2}-\frac{\theta k}{\pi}\right)\frac{1}{\tau}+\left[\frac{3}{8}-\frac{\theta k}{2\pi}+\frac{\theta k^2}{2\pi}\left(\frac{\theta}{\pi}+1\right)\right]\frac{1}{\tau^2}+\ldots\right\} \tag{33}$$

In order for the flow in the physical ζ plane to be continuous across lines AD and CD, the transformation function Eq. (32) cannot have a branch point at infinity. In other words, the term containing $1/\tau$ on the right-hand side of Eq. (33) must vanish. Thus

$$k = \pi/2\theta \tag{34}$$

and the derivative has a simplified form

$$\frac{d\zeta}{d\tau} = b\left(1 + \frac{1+k}{4}\frac{1}{\tau^2} + \ldots\right) \tag{35}$$

The value of b is determined by requiring that the point C at $\tau = 1$ be mapped into the origin of the ζ plane. Thus from Eq. (32),

$$\frac{a}{b} = \int_0^1 \left(1 + \frac{k}{\tau}\right)^{-\theta/\pi} \left(\frac{\tau}{1-\tau}\right)^{1/2} d\tau \tag{36}$$

This Gaussian-type definite integral is evaluated by using the approximating formula[12]

$$\int_0^1 f(x)\left(\frac{x}{1-x}\right)^{1/2} dx = \sum_{i=1}^{n} \frac{2\pi x_i}{2n+1} f(x_i) \tag{37}$$

in which

$$x_i = \cos^2\left(\frac{2i-1}{2n+1}\frac{\pi}{2}\right) \tag{38}$$

Not too many terms are needed in the polynomial on the right side of Eq. (37) for its convergence. Satisfactory results have been obtained in our computation with $n = 10$.

Because $d\zeta/d\tau = b$ at infinity, the complex potential for the uniform flow in the τ plane is

$$W_2 = -b\tau \tag{39}$$

The residue theorem gives

$$\oint W_2 d\zeta = \oint W_2 \frac{d\zeta}{d\tau} d\tau = -2\pi i b^2 \frac{1+k}{4}$$

substitution of which into Eq. (5) yields

$$\frac{m_{22}}{\rho\pi a^2} = \left(\frac{b}{a}\right)^2 \frac{1+k}{2} - \frac{1}{\pi\tan\theta} \tag{40}$$

When $\theta = \pi/2$ the triangle becomes a flat plate. For this case $k = 1$ and $a/b = 1$, so that the right-hand side of Eq. (40) has the value of 1 as it should for a flat plate.

The A-E and W-E rules for lift on the triangular cross section are respectively

$$(m_{22}/\rho\pi a^2)_{AE} = 1/\pi\tan\theta \tag{41}$$

$$(m_{22}/\rho\pi a^2)_{WE} = 1 \tag{42}$$

They are plotted in Fig. 12 in comparison with the exact solution computed from Eq. (40).

We now turn to the sideslip problem in which the fluid motion faraway is parallel to the s axis in the ζ plane of Fig. 11a. The transformation

$$\tau_1 = \tau - (1-k)/2 \tag{43}$$

shifts the origin of coordinate axes to the middle of the line segment AC in the τ_1 plane, as indicated in Fig. 11c. In this plane, the complex potential of a uniform flow of speed b normal to the flat plate AC can be written out and then expanded into a series of τ:

$$W_1 = ib\left[\tau_1^2 - \left(\frac{1+k}{2}\right)^2\right]^{1/2} = ib\left[\tau - \frac{1-k}{2} - \frac{(1+k)^2}{8\tau} + \ldots\right] \tag{44}$$

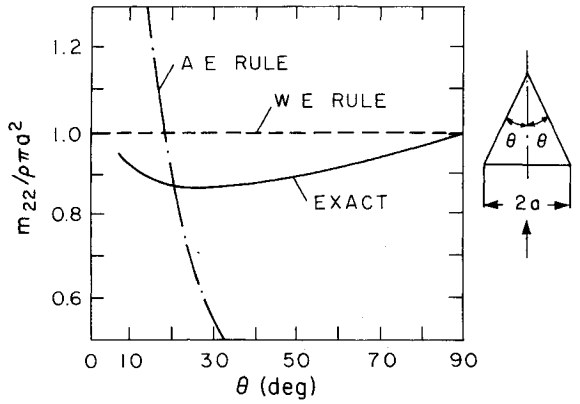

Fig. 12 Apparent-mass coefficient for isosceles triangular sections in lift problem.

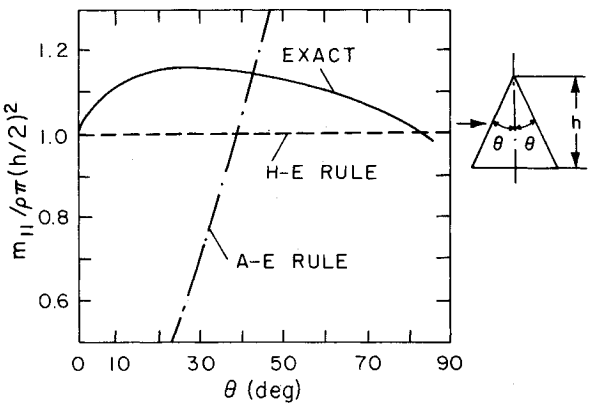

Fig. 13 Apparent-mass coefficient for isosceles triangular sections in sideforce problem.

Substitution of Eqs. (35) and (44) into Eq. (4) results in

$$\frac{m_{11}}{\rho\pi(h/2)^2} = \left(\frac{b\tan\theta}{a}\right)^2 (k^2 - 1) - \frac{4\tan\theta}{\pi} \tag{45}$$

in which the apparent-mass coefficient is made dimensionless by using that for a circle of diameter h, and k and b are still determined by Eqs. (34) and (36). The A-E and H-E rules for this case are respectively

$$\left[\frac{m_{11}}{\rho\pi(h/2)^2}\right]_{AE} = \frac{4\tan\theta}{\pi} \tag{46}$$

$$\left[\frac{m_{11}}{\rho\pi(h/2)^2}\right]_{HE} = 1 \tag{47}$$

Equations (45-47) are plotted in Fig. 13.

Conclusions on the Use of Approximation Rules

Exact expressions are obtained for apparent-mass coefficients of bodies whose cross sections are either formed by two circular arcs or have isosceles triangular shapes. To estimate lift on sections formed by two circles using the W-E rule, the maximum errors are around 10% for the case of flat-topped partial circles (Fig. 6) and about 30% for all other cases. These errors are interchanged when the H-E rule is used to estimate sideforces. Particularly good results are obtained from the H-E rule in Fig. 7 for two circles of equal radii, in Fig. 8 for the pear-shaped section, and in Fig. 9 for the body-store combination if the diameter of the store is less than 60% of that of the body. When applied to isosceles triangular sections, both W-E and H-E rules cause 15% maximum

errors. However, the errors resulting from using the A-E rule to estimate lift and sideforce are too large to make this approximating method applicable to any of the sections considered in the present work.

Although a generalized conclusion is not attempted here to include sections of arbitrary shape, it seems that special care must be taken in using the A-E rule to estimate aerodynamic forces on a fuselage.

Acknowledgment

This work of C.-Y. Chow was supported by the Air Force Office of Scientific Research under Grant AFOSR 82-0037.

References

[1] Nielsen, J.N., *Missile Aerodynamics,* McGraw-Hill, New York, 1960, Sec. 10.5.

[2] Sedov, L.I., *Two-Dimensional Problems in Hydrodynamics and Aerodynamics,* Wiley Interscience, New York, 1965, pp. 28-29.

[3] Keldysh, V.V., "Application of Slender Body Theory to the Calculation of Aerodynamic Properties of Low Aspect Ratio Wings with Nacelles at Their Tips," *Prikladnaia Matematika i Mekhanika,* Vol. 22, 1958, pp. 126-132.

[4] Portnoy, H., "The Slender Wing with a Half Body of Revolution Mounted Beneath," *The Aeronautical Journal of the Royal Aeronautical Society,* Vol. 72, Sept. 1968, pp. 803-807.

[5] Andrews, R.D., "The Lift of a Slender Combination of a Fuselage of Rectangular Cross-Section with a High Wing," *The Aeronautical Journal of the Royal Aeronautical Society,* Vol. 74, Nov. 1970, pp. 903-906.

[6] Crowell, K.R. and Crowe, C.T., "Prediction of the Lift and Moment on a Slender Cylinder-Segment Wing-Body Combination," *Aeronautical Journal,* Vol. 77, June 1973, pp. 295-298.

[7] Huang, M.-K., "Aerodynamic Interference of Wing-Body-Store Combinations," *Acta Mechanica Sinica,* No. 3, March 1979, pp. 291-293.

[8] Wolowicz, C.H. and Yancey, R.B., "Longitudinal Aerodynamic Characteristics of Light, Twin-Engine, Propeller-Driven Airplanes," NACA TN D-6800, June 1972, p. 38.

[9] Schlichting, H. and Truckenbrodt, E., *Aerodynamics of the Airplane,* McGraw-Hill, New York, 1979, Chaps. 5 and 6.

[10] Jones, R.T., "Properties of Low-Aspect-Ratio Wings at Speeds Below and Above the Speed of Sound," NACA TR-835, 1946.

[11] Bryson, A.E., "Stability Derivatives for a Slender Missile with Application to a Wing-Body-Vertical Tail Configuration," *Journal of Aeronautical Science,* Vol. 20, May 1953, pp. 297-308.

[12] Abramowitz, M. and Stegun, I.A., eds., *Handbook of Mathematical Functions with Formulas, Graphs, and Mathematical Tables,* Dover, New York, 1965, p. 889.